

# Angular Momentum Loss Mechanisms in Cataclysmic Variables below the Period Gap

Yong Shao<sup>1</sup> and Xiang-Dong Li<sup>1,2</sup>

<sup>1</sup>*Department of Astronomy, Nanjing University, Nanjing 210093, China*

<sup>2</sup>*Key laboratory of Modern Astronomy and Astrophysics (Nanjing University), Ministry of Education, Nanjing 210093, China*

*lixd@nju.edu.cn*

## ABSTRACT

Mass transfer in cataclysmic variables (CVs) is usually considered to be caused by angular momentum loss (AML) driven by magnetic braking and gravitational radiation (GR) above the period gap, and solely by GR below the period gap. The best-fit revised model of CV evolution recently by Knigge et al. (2011), however, indicates that AML rate below the period gap is  $2.47(\pm 0.22)$  times the GR rate, suggesting the existence of some other AML mechanisms. We consider several kinds of consequential AML mechanisms often invoked in the literature: isotropic wind from the accreting white dwarfs, outflows from the Lagrangian points, and the formation of a circumbinary disk. We found that neither isotropic wind from the white dwarf nor outflow from the  $L_1$  point can explain the extra AML rate, while outflow from the  $L_2$  point or a circumbinary disk can effectively extract the angular momentum provided that  $\sim (15 - 45)\%$  of the transferred mass is lost from the binary. A more promising mechanism is a circumbinary disk exerting gravitational torque on the binary. In this case the mass loss fraction can be as low as  $\lesssim 10^{-3}$ .

*Subject headings:* stars: cataclysmic variables – stars: evolution – CVs: general

## 1. Introduction

Cataclysmic variables (CVs) are short-period binaries consisting of a white dwarf star accreting material from a lower-mass main-sequence star that is overflowing its Roche-lobe (Warner 1995). In the standard model, mass transfer in CVs is driven by angular momentum

loss (AML) driven by gravitational radiation (GR) (Kraft et al. 1962) and magnetic braking (MB) (Verbunt & Zwaan 1981).

The orbital period ( $P_{\text{orb}}$ ) distribution of CVs has been summarized by Ritter & Klob (2003), which is bimodal with  $\sim 45\%$  of CVs having period in the range of  $\sim 3 - 16$  h, another  $\sim 45\%$  with  $\sim 80$  min  $- 2$  h, and the rest  $\sim 10\%$  with  $\sim 2 - 3$  h. The number of CVs in the period interval  $\sim 2 - 3$  h is small, and it is known as the period gap. In seeking a plausible explanation of the period gap in CV evolution, several authors (Rappaport et al. 1983; Spruit & Ritter 1983; Livio & Pringle 1994) proposed the “disrupted” MB models which are related to the transition of AML mechanisms. The general ideal is that, mass transfer in CVs above the period gap is primarily driven by MB at a rate rapid enough, making the secondary star out of thermal equilibrium, so that the secondary star is oversized and has larger radius than a main-sequence star with the same mass. Along with mass transfer, the secondary star loses mass gradually, and finally become fully convective when  $P_{\text{orb}} \simeq 3$  h. AML is now assumed to be caused solely by GR, because MB is vanished. Accordingly the oversized secondary star begins to shrink and underfill its Roche-lobe in attempt to reach thermal equilibrium, cutting off matter transfer. CVs becomes very faint, and virtually unobservable. When the Roche-lobe is filled again due to orbit shrinking driven by GR at  $P_{\text{orb}} \simeq 2$  h, mass transfer restarts from the secondary star.

Most recently Knigge et al. (2011) reconstructed the complete evolutionary path followed by CVs, using the observed mass-radius relationship of their secondary stars. For AML, they adopted a scaled versions of the standard GR loss rate and the Rappaport et al. (1983) MB law. With suitable normalization parameters,  $f_{GR}$  and  $f_{MB}$ , these recipes provide acceptable matches to the observed data. The best-fitting scaling factors are  $f_{GR} = 2.47 \pm 0.22$  below the gap, and  $f_{MB} = 0.66 \pm 0.05$  above, which describe the mass-radius data significantly better than the standard model ( $f_{GR} = f_{MB} = 1$ ).

Here we focus on the origin of the enhanced AML below the gap, which has already been mentioned before (e.g. Kolb & Baraffe 1999; Patterson 2001; Spruit & Taam 2001; Barker & Kolb 2003). One obvious candidate is the residual MB. Generally, the magnetic field of a low-mass star is supposed to be anchored at the interface between the convective envelope and the radiative core. For a fully convective star, such as the secondary star of CVs below the period gap, the interface disappears, and MB is thought to be closed. However, there is strong evidence that fully convective stars are capable of generating significant magnetic fields (Sills et al. 2000; Andronov et al. 2003), which might develop in a different way than low-mass main-sequence stars (for a discussion see §8.5 in Knigge et al. 2011, and references therein). At present it is not clear whether the magnetically channelled stellar winds can produce MB strong enough to be consistent with the model for CV evolution (e.g.

Li et al. 1994). In this paper we will examine other mechanisms that are needed to account for the extra AML.

During the mass transfer processes, part of the transferred mass from the secondary star may escape from the binary system, carrying away the orbital angular momentum. AML associated with mass transfer is called consequential angular momentum loss (CAML) (King & Kolb 1995). There are several types of CAML due to different way of mass loss in the CV evolution (Soberman et al. 1997): (1) isotropic wind from the accreting white dwarf and surrounding accretion disk (King & Kolb 1995), (2) outflow through the Lagrangian points  $L_1$  or  $L_2$  (Vanbeveren et al. 1998), and (3) a circumbinary (CB) disk (van den Heuvel 1994; Taam & Spruit 2001).

The organization of this paper is as follows. We introduce the basics of orbital evolution and possible CAML mechanisms in Section 2. In Section 3, we constrain possible AML mechanisms to explain the extra AML rate below the period gap. Discussions and conclusions are presented in the final Section.

## 2. Orbital evolution and CAML in CVs

We first derive the relation between the CAML rate and the mass transfer rate  $\dot{M}_2$ , following the approach in King (1988) and Knigge et al. (2011).

We assume that the total angular momentum of the binary is dominated by the orbital angular momentum,

$$J = M_1 M_2 \left( \frac{Ga}{M} \right)^{1/2}, \quad (1)$$

where  $a$  is the binary separation,  $M_1$ ,  $M_2$ , and  $M$  are the masses of the white dwarf, the secondary star, and the binary system, respectively. The relation between the binary separation  $a$  and the orbital angular velocity  $\omega$  is given by the Kepler’s third law,

$$GM = a^3 \omega^2. \quad (2)$$

Logarithmic differentiation of Eq. (1) gives

$$\frac{\dot{J}}{J} = \frac{\dot{M}_1}{M_1} + \frac{\dot{M}_2}{M_2} + \frac{\dot{a}}{2a} - \frac{\dot{M}}{2M}. \quad (3)$$

The obital AML rate in CVs contains two items. One is the systemic AML due to MB and/or GR; the other is CAML, which is related to the mass transfer rate. So the total obital AML rate can be written as

$$\dot{J} = \dot{J}_{sys} + \dot{J}_{CAML}. \quad (4)$$

When mass is transferred from the donor star to the white dwarf, we assume that a fraction  $\delta$  of the matter flow escapes from the CV binary, i.e.,

$$\dot{M} = \delta \dot{M}_2, \quad (5)$$

which means that the actual accretion rate of the white dwarf is

$$\dot{M}_1 = (\delta - 1) \dot{M}_2. \quad (6)$$

Considering that the CAML rate is related to the mass transfer rate  $\dot{M}_2$ , we can write

$$\frac{\dot{J}_{CAML}}{J} = \nu \frac{\dot{M}_2}{M_2}, \quad (7)$$

where  $\nu$  is a parameter as a function of  $\delta$  (Knigge et al. 2011). In order to eliminate  $\dot{a}/a$  in Eq. (3), we use the Paczynski (1971) formula for the Roche-lobe radius  $R_L$  of the donor star,

$$R_L = 0.462 (M_2/M)^{1/3} a. \quad (8)$$

Logarithmic differentiation of Eq. (8) yields

$$\frac{\dot{R}_L}{R_L} = \frac{\dot{M}_2}{3M_2} - \frac{\dot{M}}{3M} + \frac{\dot{a}}{a}. \quad (9)$$

For a Roche-lobe-filling donor star with steady mass transfer, variation of the stellar radius  $R_2$  and the Roche-lobe radius  $R_L$  should be in step, i.e.,

$$\frac{\dot{R}_L}{R_L} = \frac{\dot{R}_2}{R_2}. \quad (10)$$

To deal with  $\dot{R}_2$ , we use the mass-radius relation  $R_2 = M_2^\zeta$  and its logarithmic differentiation

$$\frac{\dot{R}_2}{R_2} = \zeta \frac{\dot{M}_2}{M_2}, \quad (11)$$

where  $\zeta$  is the mass-radius exponent. Knigge et al. (2011) showed that after a CV donor emerges from the bottom of the period gap, the exponent  $\zeta$  evolves from  $\simeq 0.8$  (in thermal equilibrium) to  $\simeq 1/3$  at the minimum period, and finally to  $\simeq -1/3$  (see also Rappaport et al. 1982). They adopted broken-power-law fit to the updated  $M_2 - R_2$  data in Knigge (2006), with  $\zeta = 0.3$  for  $M_2 \lesssim 0.07 M_\odot$ , and  $\zeta = 0.61$  for  $0.07 M_\odot \lesssim M_2 \lesssim 0.2 M_\odot$ . Here  $0.2 M_\odot$  and  $0.07 M_\odot$  are the secondary masses just below the gap and at the minimum period where the secondary stars become degenerate and the orbital periods start to bounce back into the period-increasing phase, respectively. Adopt  $q = M_2/M_1$  and typical white dwarf mass

$M_1 = 0.6M_\odot$  in CVs,  $\zeta$  decreases from  $\sim 0.61$  to  $\sim 0.3$  with decreasing  $q$ . In the following we calculate  $\zeta$  by using the  $M(R)$  relation derived from numerical calculations of CV binary evolution, which is very close to the empirical one in Knigge et al. (2011).

Combining Eqs. (3)-(11), one can derive

$$\frac{\dot{M}_2}{M_2} = \frac{\dot{J}_{sys}}{JD}, \quad (12)$$

where

$$D = (5/6 + \zeta/2) - \frac{M_2}{M_1} + \delta\left(\frac{M_2}{M_1} - \frac{M_2}{3M}\right) - \nu. \quad (13)$$

Here the systemic AML mechanism below the gap is GR, and its rate is given by (Landau & Lifshitz 1951)

$$\frac{\dot{J}_{GR}}{J} = -\frac{32}{5} \frac{G^3}{c^5} M_1 M_2 a^{-4} \quad (14)$$

Next we consider the possible CAML mechanisms. For isotropic wind (e.g., outflows due to nova explosions and/or wind emanating from the accretion disk), we assume that it carries the white dwarf's specific obital angular mometum  $j_1$ ,

$$j_1 = \frac{M_2}{M_1 M} J. \quad (15)$$

For outflows from the Lagrangian point  $L_2$  the specific obital angular mometum is

$$j_2 = a_{L_2}^2 \omega, \quad (16)$$

where  $a_{L_2}$  is the distance between the mass center of binary and the  $L_2$  point. Finally for CB disks we assume that it extracts the orbital angular momentum from the binary by tidal force. The specific obital angular momentum  $j_3$  is given by,

$$j_3 = \gamma a^2 \omega \quad (17)$$

where  $\gamma^2 a$  is taken as the inner radius of the CB disk. Usually,  $\gamma = 1.5$  (Soberman et al. 1997).

### 3. Constraining the CAML machanisms below the period gap

The best-fit revised model of CV evolution in Knigge et al. (2011) indicates that the AML rate below the period gap is  $2.47\dot{J}_{GR}$ . This means that some other AML machanisms besides GR should work. In the following we will discuss the feasibility of the AML related to isotropic wind, outflow from  $L_2$  point, and CB disks, respectively.

### 3.1. Isotropic wind

Combining Eqs. (5), (7) and (15), we can derive the obital AML rate,  $\dot{J}_{CAML,1}$  of isotropic wind as

$$\frac{\dot{J}_{CAML,1}}{J} = \delta \frac{M_2^2}{M_1 M} \frac{\dot{M}_2}{M_2}, \quad (18)$$

and hence

$$\nu = \delta \frac{M_2^2}{M_1 M}. \quad (19)$$

Let  $\dot{J}_{CAML,1} = 1.47 \dot{J}_{GR}$  and combined Eqs. (12)-(14) and (18)-(20), we have

$$\frac{2.47}{1.47} \frac{\delta M_2^2}{M_1 M} = (5/6 + \zeta/2) - \frac{M_2}{M_1} + \delta \left( \frac{M_2}{M_1} - \frac{M_2}{3M} \right), \quad (20)$$

which can be transformed into

$$\delta \simeq \frac{(2.5 + 1.5\zeta - 3q)(1 + q)}{2q(q - 1)}. \quad (21)$$

For CVs below the period gap,  $0 < q < 0.33$ ,  $\zeta > 0$ , so  $\delta$  is always negative, indicating that the isotropic wind cannot provide the extra  $1.47 \dot{J}_{GR}$  AML. This conclusion remains valid if we let most of the material to escape from the  $L_1$  point (Barker & Kolb 2003).

### 3.2. Outflow from the $L_2$ point

Similar as in section 3.1, we derive the obital AML rate,  $\dot{J}_{CAML,2}$ , of outflow from the  $L_2$  point by combining Eqs. (5) and (16),

$$\frac{\dot{J}_{CAML,2}}{J} = \delta \frac{a_{L_2}^2}{a^2} \frac{M}{M_1} \frac{\dot{M}_2}{M_2}, \quad (22)$$

which gives

$$\nu = \delta \frac{a_{L_2}^2}{a^2} \frac{M}{M_1}. \quad (23)$$

Then we obtain the following relation

$$\frac{2.47}{1.47} \frac{\delta a_{L_2}^2 M}{a^2 M_1} = (5/6 + \zeta/2) - \frac{M_2}{M_1} + \delta \left( \frac{M_2}{M_1} - \frac{M_2}{3M} \right). \quad (24)$$

After simplification we have

$$\delta \simeq \frac{(2.5 + 1.5\zeta - 3q)(1 + q)}{5(1 + q)^2 x^2 - q(2 + 3q)}, \quad (25)$$

where  $x = a_{L_2}/a$ . For different  $q$ , the values of  $x$  are given in Mochnacki (1984). The relation between  $\delta$  and  $q$  is shown in Figure 1. It is seen that the required value of  $\delta$  ranges from  $\sim 0.15$  to  $\sim 0.45$ .

### 3.3. CB disks

The origin of the CB disks may stem from the remnant of the late stage of the common envelope evolution phase that formed the CVs, or matter outflow from CVs during the mass transfer processes (Taam & Soudquist 2000). Through tidal interaction of the CB disk and CVs binary, the CB disk can extract orbital angular momentum from binary if part of the transferred mass flows into the disk rather than onto the white dwarf. The corresponding AML rate is,

$$\dot{J}_{CAML,3} = \delta \gamma \dot{M}_2 a^2 \omega. \quad (26)$$

Then we can derive

$$\delta \simeq \frac{(2.5 + 1.5\zeta - 3q)(1 + q)}{7.56(1 + q)^2 - q(2 + 3q)}. \quad (27)$$

The relation between  $\delta$  and  $q$  is shown in Figure 2. The value of  $\delta$  lies between  $\sim 0.22$  and  $\sim 0.4$ , comparable with that in the case of outflow from the  $L_2$  point.

The above result is under the assumption that AML is only caused by mass loss. Actually there is gravitational torque between the CB disk after it is formed and the binary, which is more efficient to extract angular momentum from the binary (Spruit & Taam 2001). The AML rate under this torque can be expressed as

$$\dot{J}_{CB} = \gamma \left( \frac{2\pi a^2}{P_{\text{orb}}} \right) \delta \dot{M}_2 \left( \frac{t}{t_{vi}} \right)^{1/3}, \quad (28)$$

where  $t$  is the time since mass transfer begins, and  $t_{vi}$  is the viscous timescale at the inner edge of the CB disk, given by  $t_{vi} = 2\gamma^3 P_{\text{orb}} / 3\pi\alpha\beta^2$ , where  $\alpha$  is the viscosity parameter (Shakura & Sunyaev 1973), and  $\beta$  is the ratio of the scale height to the radius of the disk. Equation (28) can be further simplified to be

$$\dot{J}_{CB} = A(GM)^{2/3} \delta \dot{M}_2 t^{1/3}, \quad (29)$$

where  $A = (3\alpha\beta^2/4)^{1/3}$ . Similar as the derivation of Eq. (20), we obtain the following relation for the CB disk,

$$\frac{2.47}{1.47} \frac{AG^{1/6} M^{7/6} \delta t^{1/3}}{M_1 a^{1/2}} = (5/6 + \zeta/2) - \frac{M_2}{M_1} + \delta \left( \frac{M_2}{M_1} - \frac{M_2}{3M} \right). \quad (30)$$

Previous investigations (Taam & Spruit 2001; Taam et al. 2003; Willems et al. 2005) suggest that very small values of  $\delta (\ll 1)$  are required for CV evolution. Thus the third term on the rhs of Eq. (30) can be neglected. Considering the fact that  $\zeta/2$  and  $q$  also roughly counteract each other, and  $M \sim M_1$ , Eq. (30) is changed to be

$$\begin{aligned} \delta &\simeq \frac{1}{2A(2\pi)^{1/3}} \left( \frac{P_{\text{orb}}}{t} \right)^{1/3} \\ &\sim 8 \times 10^{-4} \alpha_{0.01}^{-1/3} \beta_{0.03}^{-2/3} \left( \frac{P_{\text{orb},2}}{t_9} \right)^{1/3}, \end{aligned} \quad (31)$$

where  $\alpha_{0.01} = \alpha/0.01$ ,  $\beta_{0.03} = \beta/0.03$  (Belle et al. 2004),  $P_{\text{orb},2} = P_{\text{orb}}/2$  hr, and  $t_9 = t/10^9$  yr. This is close to the result  $\delta \sim 3 \times 10^{-4}$  adopted in the numerical calculations by Taam et al. (2003) for CV evolution.

To investigate the effect on AML of the uncertainties in treatment of CB disks we have numerically solved Eq. (30). Figures 3 and 4 show the calculated values of  $\delta$  as a function of  $q$  for different values of  $\alpha$  and  $\beta$ . It is seen that generally smaller  $\alpha$  or  $\beta$  corresponds to larger  $\delta$ . This is easy to understand with Eq. (29): smaller  $\alpha$  or  $\beta$  indicates less efficient angular momentum transfer within the disk, which requires more mass input into the CB disk to guarantee enough AML from the orbit. Nevertheless, the values of  $\delta$  are always small ( $< a$  few  $10^{-3}$ ) when we change  $\alpha$  from 0.001 to 0.1, and  $\beta$  from 0.005 to 0.1. This implies that CB disks are indeed very efficient in draining orbital angular momentum through gravitational torques even with a very small mass input rate.

To show how CB disks can influence the evolution of CVs below the gap, we have also performed binary evolution calculations adopting an updated version of the stellar evolution code developed by Eggleton (1971, 1972) (see also Han et al. 1994; Pols et al. 1995). We set initial solar chemical compositions (i.e.,  $X = 0.7$ ,  $Y = 0.28$ , and  $Z = 0.02$ ) for the donor star, and take the ratio of mixing length to the pressure scale height to be 2.0, and the convective overshooting parameter to be 0.12.

We follow the evolution of a CV just below the gap with a donor star of mass  $0.2M_{\odot}$  and an orbital period  $\sim 0.1$  d. For CB disks we take  $A\delta$  as one free parameter to assess its influence on the evolution of CVs, since  $\alpha$ ,  $\beta$  and  $\delta$  are always combined together in evaluating the AML rate (see Eq. [29]). For typical values of  $\alpha(= 0.01)$  and  $\beta(= 0.03)$  (Taam et al. 2003, and references therein),  $A \simeq 0.02$ . Considering the fact that suitable value of  $\delta$  may range from  $\sim 10^{-7}$  to a few  $10^{-4}$  (Taam et al. 2003; Willems et al. 2005), we constrain the adopted value of  $A\delta$  to be less than  $\sim 10^{-5}$ . Larger  $A\delta$  may cause unstable mass transfer. The stability of mass transfer can be examined by comparing the Roche-lobe radius exponent  $\zeta_L$  due to mass loss with  $\zeta$  (Soberman et al. 1997), which are shown in Figure 5 as a function of  $q$ . From top to bottom, the solid curves represent  $\zeta_L$  with  $A\delta$  ranging from  $5 \times 10^{-5}$  to  $1 \times 10^{-5}$  in steps of  $1 \times 10^{-5}$ , and the dashed lines show the mass-radius exponent  $\zeta$  of 0.8,  $1/3$ , and  $-1/3$ , respectively. Since the mass transfer would be unstable when  $\zeta_L \geq \zeta$ , we can derive that  $A\delta$  should be  $\lesssim (2 - 3) \times 10^{-5}$  to guarantee stable mass transfer.

In Figure 6 we present examples of the evolutionary sequences of the donor mass, orbital period, mass transfer rate, and the ratio of total AML rate and the AML rate due to GR ( $N \equiv \dot{J}/\dot{J}_{GR}$ ) to show the influence CB disks. The panels from top to bottom correspond to  $A\delta = 0$  (i.e., AML due to GR sololy),  $4 \times 10^{-6}$ ,  $9 \times 10^{-6}$  and  $2 \times 10^{-5}$ , respectively. When  $A\delta = 4 \times 10^{-6}$  (or  $\delta = 2 \times 10^{-4}(A/0.02)^{-1}$ ), the evolution seems similar to that with GR only.



However, the mass transfer processes are actually accelerated, with  $\sim 10\%$  higher average mass transfer rate and  $\sim (10 - 15)\%$  higher AML rate than in the GR-only case. This tendency becomes more intense when  $A\delta$  goes up. When  $A\delta = 2 \times 10^{-5}$ , the average mass transfer rate is enhanced by  $\sim 70\%$ , and the AML rate  $\dot{J}$  becomes  $\sim 2 - 3$  times  $\dot{J}_{GR}$ . These results imply that a tiny fractional input rate ( $\delta \lesssim 10^{-3}$ ) into CB disks can significantly change the evolution. This is in contrast with mass loss-assisted AML mechanisms, which usually require a much larger fraction of the transferred mass to leave the binary system (although in real situation there might be multiple mechanisms work simultaneously).

#### 4. Discussion and Conclusions

The secular evolution of CVs is thought to be driven by the AML. Two mechanisms usually invoked to account for the dissipation of AM are GR and MB of the secondary star. However, this dual loss-mechanism cannot completely account for the magnitudes of the mass-transfer rates inferred for some CVs, and for the large spread in the mass transfer rates observed at a given orbital period (e.g. Spruit & Taam 2001). Likely additional AML mechanisms include mass loss from the binary during the mass transfer process, which carries away the orbital angular momentum from the binary. Below the period gap in CVs evolution, AML mechanism was usually considered to be driven by solely GR, while the best-fit result with observations indicates that AML rate is about  $2.47\dot{J}_{GR}$  (Knigge et al. 2011). This offers a possibility to constrain the AML mechanisms besides GR. We consider several kinds of CAML mechanisms often invoked in the literature: isotropic wind from the accreting white dwarfs, outflows from the Lagrangian points, and the formation of a CB disk.

We found that neither isotropic wind from the white dwarf nor outflow from the  $L_1$  point can explain the extra  $1.47\dot{J}_{GR}$  AML rate, while outflow from the  $L_2$  point or a CB disk is more effective in extracting the angular momentum. For a  $0.6M_{\odot}$  white dwarf, the fraction  $\delta$  of mass loss in the total transferred mass is  $\sim 0.15 - 0.45$  or  $\sim 0.2 - 0.40$ , respectively. Actually it is found that  $\delta$  is always less than 0.45 for different mass of the white dwarf in our calculations. Note that when mass is lost from the  $L_2$  point, it is very likely to form a CB disk around the binary (van den Heuvel 1994), so it is not surprised that the values of  $\delta$  are very close in these two cases.

When the tidal interaction between the CB disk and the binary is included, the mass transfer rate can be enhanced much more efficiently, and a very small fraction ( $\delta \lesssim 10^{-3}$ ) of mass loss is required. This will suggest a much lighter CB disk than in the former cases. The CB disks are thought to be large (up to several AU in radius) and cool (a few thousand K at the inner edge to less than 1000 K at the outer edge), with peak emission in the

infrared (Dubus et al. 2002). Although detection of excess infrared emission from magnetic CVs provides observational support for the presence of cool gas (and possibly a CB disk) surrounding CVs (Howell et al. 2006; Dubus et al. 2007; Brinkworth et al. 2007; Hoard et al. 2007), there are still many open questions associated with the formation of the CB disks. Future observations with the measurement of the disk masses might distinguish the ways of angular momentum transfer between the CB disk and the CV binary.

We are grateful to an anonymous referee for helpful comments. This work was supported by the Natural Science Foundation of China (under grant numbers 10873008 and 11133001), and the Ministry of Science and the National Basic Research Program of China (973 Program 2009CB824800).

## REFERENCES

- Andronov, N., Pinsonneault, M., & Sills, A. 2003, *ApJ*, 582, 358
- Barker, J., & Kolb, U. 2003, *MNRAS*, 340, 623
- Belle, K. E., Sanghi, N., Howell, S. B., Holberg, J. B., & Williams, P. T. 2004, *AJ*, 128, 448
- Brinkworth, C. S., et al. 2007, *ApJ*, 659, 1541
- Dubus, G., Taam, R. E., Hull, C., Watson, D. M., & Mauerhan, J. C. 2007, *ApJ*,
- Dubus, G., Taam, R. E., & Spruit, H. C. 2002, *ApJ*, 569, 395
- Eggleton P. P., 1971, *MNRAS*, 151, 351
- Eggleton P. P., 1972, *MNRAS*, 156, 361
- Han Z., Podsiadlowski P., & Eggleton P. P., 1994, *MNRAS*, 270, 121
- Hoard, D. W., Howell, S. B., Brinkworth, C. S., Ciardi, D. R., & Wachter, S. 2007, *ApJ*, 671, 734
- Howell, S. B., et al. 2006, *ApJ*, 646, L65
- Ivanova, N., & Taam, R. E. 2003, *ApJ*, 599, 516
- King, A. R. 1988 *QJRAS*, 29, 1
- King, A. R., & Kolb, U. 1995, *ApJ*, 439, 330

- King, A. R. 1988 QJRAS,29,1
- Knigge, C. 2006, MNRAS, 373, 484
- Knigge, C., Baraffe, I., & Patterson, J. 2011, ApJS, 194, 28
- Kolb, U., & Baraffe, I. 1999, MNRAS, 309, 1034
- Kraft, R.P., Mathews, J., & Greenstein, J.L. 1962, ApJ. 136, 312
- Landau, L.D., Lifshitz, E.M. 1951, The Classical Theory of Fields, Addison-Wesley Press, Inc.
- Li, J. K., Wu, K. W., & Wickramasinghe, D. T. 1994, MNRAS, 268, 61
- Livio, M., & Pringle, J.E. 1994, APJ, 427, 956
- Mochnecki, S. W. 1984, ApJS, 55, 551
- Paczynski, B. 1971 ARA&A ,9 ,183
- Patterson, J. 2001, PASP, 113, 736
- Pols O., Tout C. A., Eggleton P. P., & Han, Z., 1995, MNRAS, 274, 964
- Rappaport, S., Joss, P. C., & Webbink, R. F. 1982, ApJ, 254, 616
- Rappaport, S., Verbunt, F., & Joss, P. C. 1983, ApJ, 275, 713
- Ritter H., & Kolb, U. 2003, A&A, 404, 301
- Ritter, H. 2008, New Astron. Rev., 51, 869
- Shakura, N. I., & Sunyaev, R. A. 1973, A&A, 24, 337
- Sills, A., Pinsonneault, M. H., & Terndrup, D. M. 2000, ApJ, 534, 335
- Soberman, G. E., Phinney, E. S., & van den Heuvel, E. P. J. 1997, A&A, 327, 620
- Spruit, H.C., & Ritter, H. 1983, A&A, 124, 267
- Spruit, H. C., & Taam, R. E. 2001, ApJ, 548, 900
- Taam, R.E., & Sandquist, E.L. 2000, ARA&A, 38, 113
- Taam, R. E., Sandquist, E. L., & Dubus, G. 2003, ApJ, 592, 1124

- Taam, R. E., & Spruit, H. C. 2001, ApJ, 561, 329
- van den Heuvel, E .P. J. 1994, in Interacting Binaries (Saas-Fee 22), Shore, S.N., et al., eds., p263
- Vanbeveren, D., Van Rensbergen, W., & De Loore, C., 1998b, in The Brightest Binaries, Kluwer Academic Pub., Dordrecht
- Verbunt, F. & Zwaan, C. 1981, A&A, 100, L7
- Warner, B. 1995, Cataclysmic Variable Stars, Cambridge University Press, Cambridge
- Webbink, R. F. 1979, in: Changing Trends in Variable Star Research, F. M. Bateson, J. Smak, & I.H. Ulrich (eds.), IAU Coll. No.46, Univ. Waikato, Hamilton, N.Z., p. 102
- Webbink, R. F. 1985, in Interacing Binary Stars, ed. J. E. Pringle & R. A. Wade(Cambridge: Cambridge University Press), 39
- Willems, B., Kolb, U., Sandquist, E. L., Taam, R. E., & Dubus, G. 2005, ApJ, 635, 1263

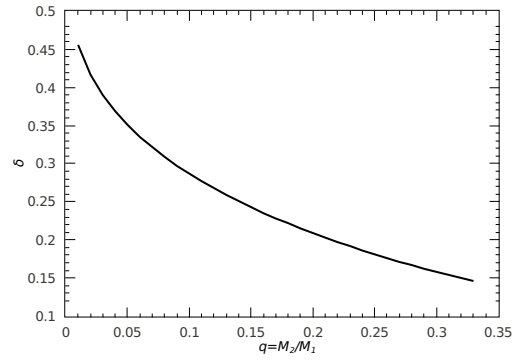


Fig. 1.— The relation between  $\delta$  and  $q$  in the case of outflow through the  $L_2$  point.

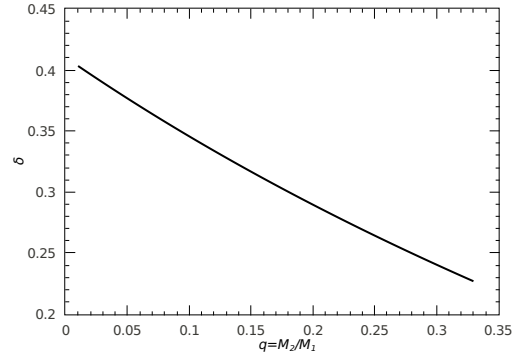


Fig. 2.— The relation between  $\delta$  and  $q$  in the case of CB disks.

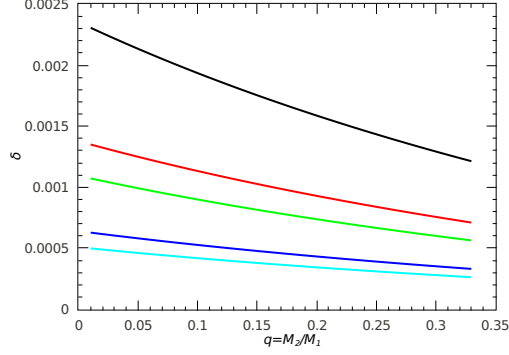


Fig. 3.— The fractional mass input rate,  $\delta$ , as a function of  $q$  for CB disks with gravitational interaction with the binary. Here we take  $\beta = 0.03$ , and the curves from top to bottom correspond to  $\alpha = 0.001, 0.005, 0.01, 0.05$ , and  $0.1$ , respectively.

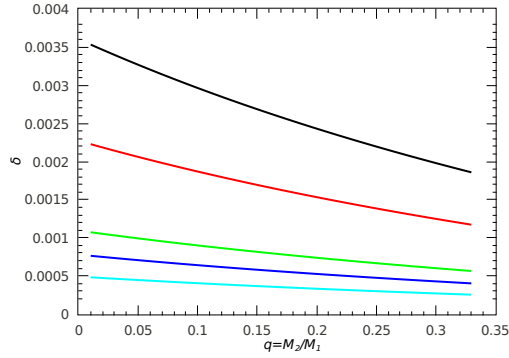


Fig. 4.— The fractional mass input rate,  $\delta$ , as a function of  $q$  for CB disks with gravitational interaction with the binary. Here we take  $\alpha = 0.01$ , and the curves from top to bottom correspond to  $\beta = 0.005, 0.01, 0.03, 0.05$ , and  $0.1$ , respectively.

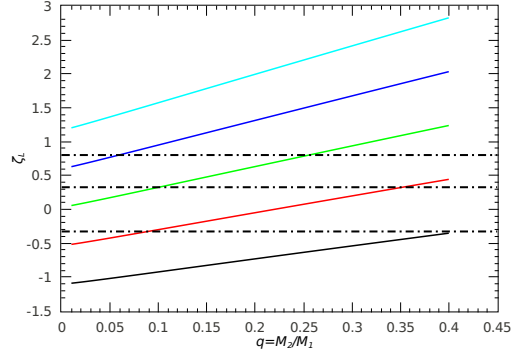


Fig. 5.— The Roche-lobe radius exponent  $\zeta_L$  as a function of  $q$ . The five solid curves represent  $\zeta_L$  with different  $A\delta$  from  $5 \times 10^{-5}$  to  $1 \times 10^{-5}$  in steps of  $1 \times 10^{-5}$  (from top to bottom). The dashed lines from top to bottom correspond to the mass-radius exponent  $\zeta = 0.8$ ,  $1/3$ , and  $-1/3$ , respectively.

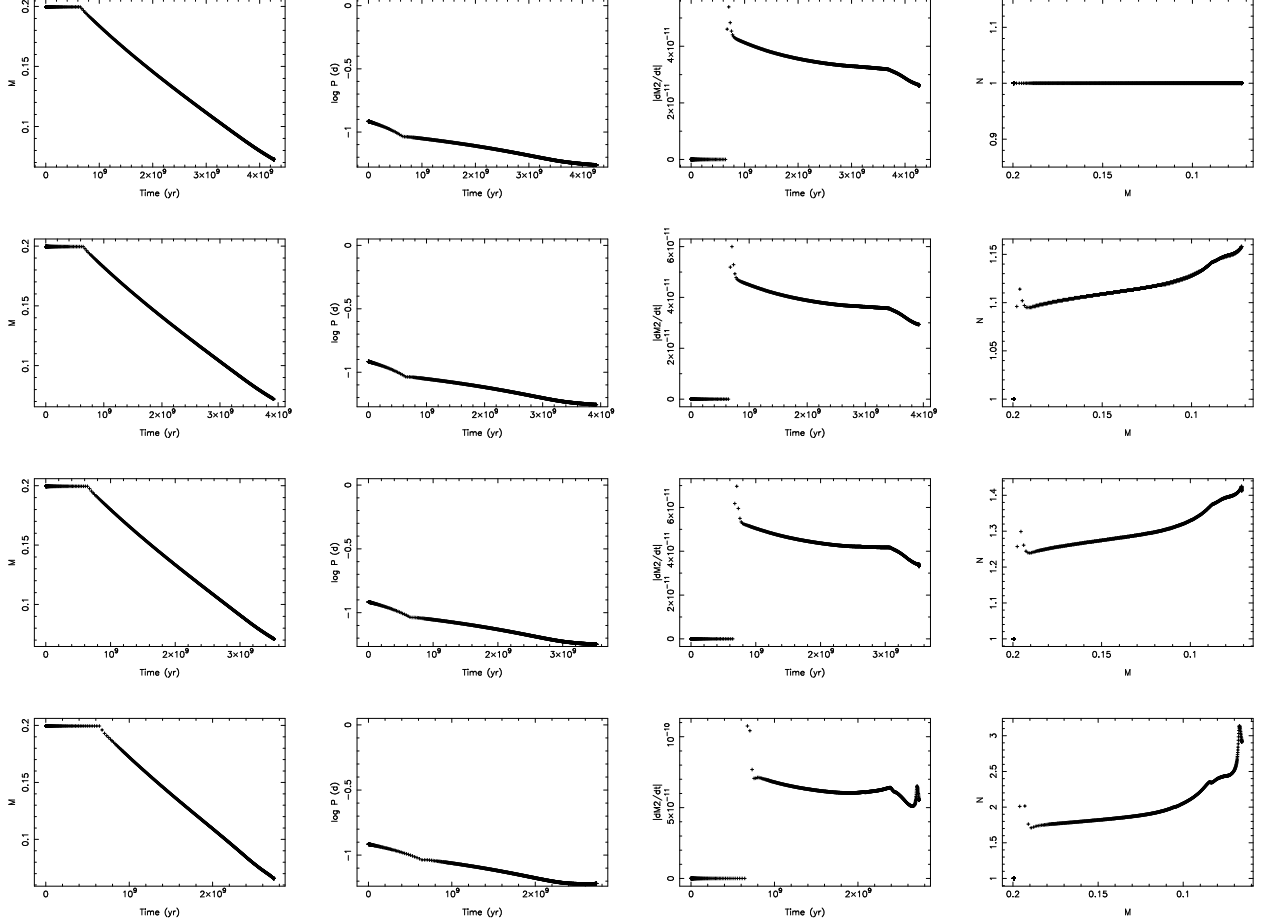


Fig. 6.— Evolution of the donor mass ( $M_\odot$ ), orbital period ( $d$ ), mass transfer rate ( $M_\odot \text{yr}^{-1}$ ), and the ratio ( $N$ ) of total AML rate and the AML rate due to GR. The panels from top to bottom correspond to AML due to GR sololy, and both GR and CB disks with  $A\delta = 4 \times 10^{-6}$ ,  $9 \times 10^{-6}$ , and  $2 \times 10^{-5}$ , respectively.